Физика и техника полупроводников, 1999, том 33, вып. 9

Optical spectra of wide band gap $Be_xZn_{1-x}Se$ alloys

© A.M. Mintairov[*,≠][¶], F.C. Peiris[+], S. Lee[+], U. Bindley[+], J.K. Furdyna[+],
S. Raymond[*], J.L. Merz[*], V.G. Melehin[≠], K. Sadchikov[≠]

[*] Department of Electrical Engineering, University of Notre Dame ,
Notre Dame, IN 46556, USA
[+] Department of Physics, University of Notre Dame,
Notre Dame, IN 46556, USA
[≠] A.F. Ioffe Physicotechnical Institute , Russian Academy of Sciences,
194021 St. Petersburg, Russia

(Получена 1марта 1999 г. Принята к печати 2 марта 1999 г.)

We report optical measurements (photoluminescence, Raman scattering, and infrared reflectance) of direct band gap and of optical phonon energies of $Be_xZn_{1-x}Se$ alloys grown by MBE on (001) GaAs substrates for a wide range of Be concentrations. The high band gap of BeSe (5.15 eV) suggests the possibility of using isoternary alloys for ultra-violet optoelectronic applications. And $Be_xZn_{1-x}Se$ has the inuque advantage that it can be lattice matched to Si at about $x = 0.5$.

We observed a strong linear shift of the $Be_xZn_{1-x}Se$ direct band gap to higher energies with increasing Be content (up to 3.63 eV for $x = 0.34$). Furthermore, optical phonon parameters for the entire range of BeSe content have been obtained. Finally, polarized infra-red and Raman spectra revealed local atomic ordering (anti-clustering) effects in the group-II sublattice.

Introduction

Be-chalcogenide semiconductor alloys have been recently proposed for improving the performance of ZnSe-based blue lasers [1]. It is expected that the incorporation of beryllium will lead to bond strengthening within the II–VI lattice, and also will increase the energy of stacking-fault formation, thus reducing defect propagation that has been seriously limiting the lifetimes of ZnSe-based devices. There are also other important opportunities for Be-chalcogenides. The high band gap of BeSe (5.15 eV) suggests the possibility of using these materials for ultra-violet (UV) optoelectronic applications. And $Be_xZn_{1-x}Se$ has the unique advantage that in can be lattice matched to Si at about $x = 0.5$. In the present paper we report optical measurements (photoluminesce, Raman scattering, and infrared (IR) reflectance) of the direct band gap and of optical photon energies of $Be_xZn_{1-x}Se$ alloys for a wide range of Be concentrations.

1. Experiment

The $Be_xZn_{1-x}Se$ ($0 < x \leq 1$) samples used in this study were grown by molecular-beam epitaxy (MBE) on (001) GaAs substrates at 310°C. The thickneses of the samples were between $0.3-1\,\mu$m. During the growth process the surface reconstruction was monitored by reflection high-energy electron diffraction (RHEED), which indicated a "streaky" pattern for all Be concentrations. The Be content of the alloys was determined from lattice parameter measurements by *x*-ray diffraction.

Photoluminescence (PL) spectra were excited by the 325 nm line (10 mW power) of a HeCd laser, and measured using 270 mm focal length monochromator equipped with a CCD detector.

IR reflectance spectra were taken at oblique incidence (10 to 50°) with a Bruker IFS-66V spectrometer. The photon frequencies and damping were extracted using a standard modeling procedure of the reflectivity spectra via multi-mode representation of the alloy dielectric function.

The Raman spectra were obtained with the argon ion laser line excitation using 514.5 nm line, and measured at 300 K using a DFS-52 double monochromator. The *xy* and *xx* components of the Raman spectra (where the $x \parallel [100]$ and $y \parallel [010]$) excited from the (001) growth plane were analyzed.

2. PL spectra

PL spectra were used to measure the direct band gap energy of $Be_xZn_{1-x}Se$ from $x = 0$ to 0.34. As in the case of pure ZnSe epitaxial layers [2], the low temperature PL spectra of $Be_xZn_{1-x}Se$ were dominated by a free exciton (FX) line and a broad deep level (*DL*) band (see Fig. 1). For low *x* (0.03, 0.09, and 0.15), donor-acceptor pair (*DAP*) transition bands having a *LO* phonon replica (for $x = 0.03$) are also clearly resolved. Due to the increasing of the halfwidth of the FX line with increasing BeSe content (from 12 meV for $x = 0.03$ up to 40 meV for $x = 0.34$), the *DAP* transition for higher *x* (0.29 and 0.34) appears as a weak shoulder at the low energy side of the FX line. We observed a strong suppression of the *DL* emission for $x > 0.3$, indicating improvement of the quality of the material.

Increasing the Be content results in a strong shift of the FX line toward to higher energies. As an example, for $x = 0.34$ the FX line was observed at an energy as high as 3.63 eV. Fig. 2 shows the FX line position

---

[¶] E-mail: Alexander.Mintairov.l@nd.edu

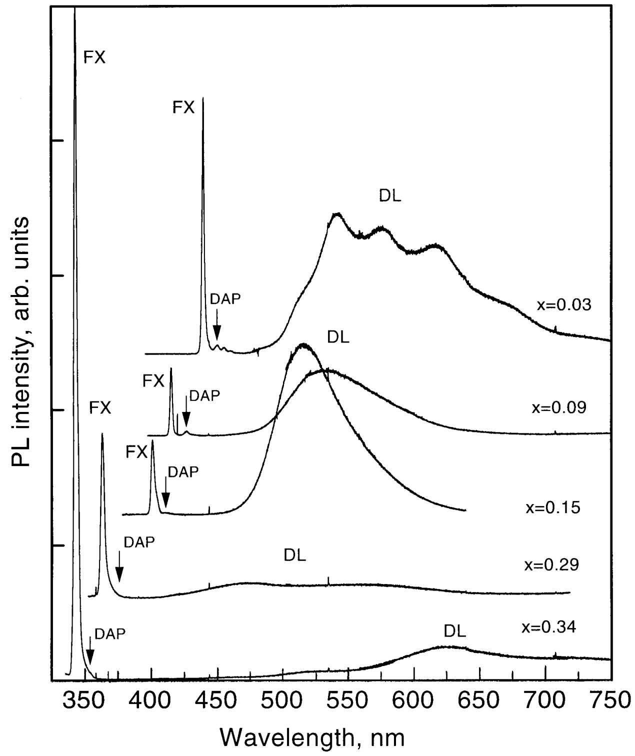

Figure 1. 10 K PL spectra of Be$_x$Zn$_{1-x}$Se ($x = 0.03$, 0.09, 0.15, 0.29 and 0.34) grown on GaAs.

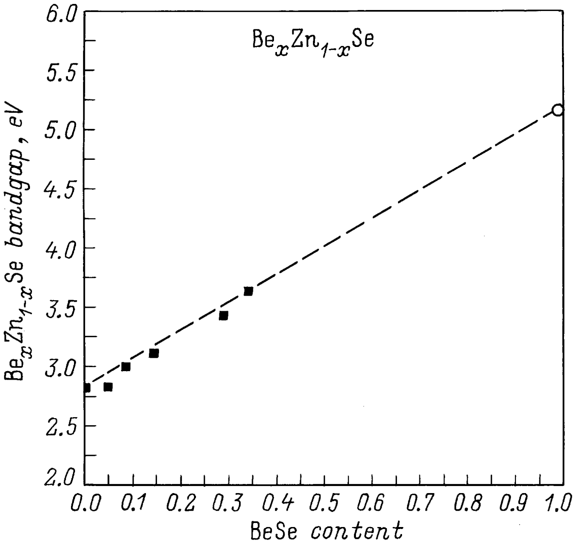

Figure 2. Be$_x$Zn$_{1-x}$Se band gap: solid squares — 10 K PL spectra; open circle — 300 K reflectivity data from Ref. [13]; dotted line — linear extrapolation from ZnSe to BeSe.

versus BeSe content, including BeSe direct band energy measured in [3] by reflectance spectroscopy. Note that all experimental points are close to the straight line connecting ZnSe and BeSe band gaps, indicating negligible bowing.

3. Phonon modes of Be$_x$Zn$_{1-x}$Se

IR (Fig. 3) and Raman (Fig. 4) spectra reveal three polar optic phonon modes of the Be$_x$Zn$_{1-x}$Se lattice for $0.01 < x < 0.08$ (Fig. 5). They are denoted on Figs. 3, 4 and 5 as TO_{1a}, TO_{2a}, TO_{2b} (transversal components) and LO_{1a}, LO_{2a}, LO_{2b} (longitudinal components). We identify two of these (subscripts $2a$ and $2d$) appearing in the frequency range 400–570 cm^{-1} as BeSe-type modes and one (subscript $1a$) appearing at 200–250 cm^{-1} as a ZnSe-type mode. For $x < 0.6$ we also identify a weak polar mode A at ~ 190 cm^{-1}, which can be attributed to ZnSe-type vibration. The ZnSe-type TO_{1a} mode shows an

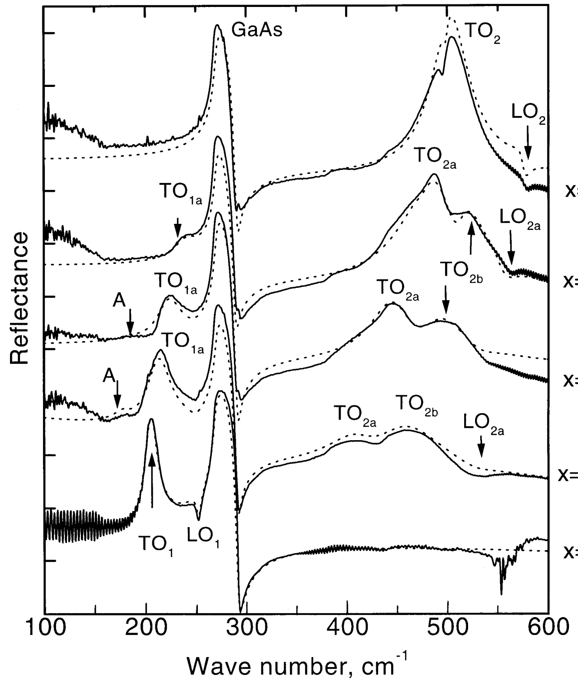

Figure 3. IR spectra of Be$_x$Zn$_{1-x}$Se ($x = 0$, 0.23, 0.57, 0.81 and 1) measured at 40° angle of incidence: solid curve — experiment, dotted curve — modeling.

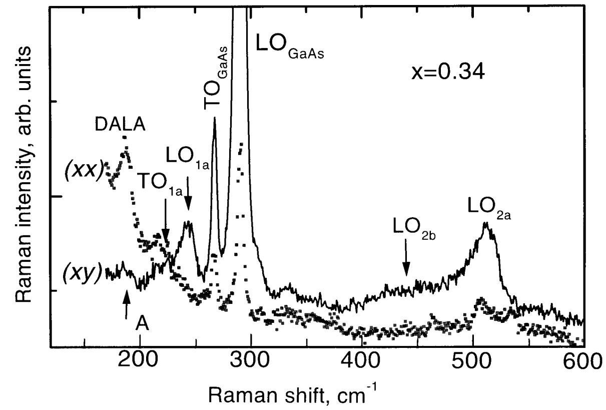

Figure 4. Raman spectra of Be$_{0.34}$Zn$_{0.66}$Se measured in xy (solid curve) and xx (dotted curve) configurations.

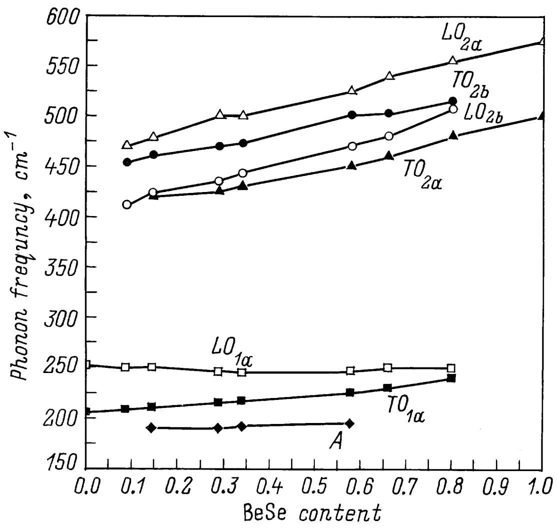

Figure 5. Dependence polar optic phonon frequencies on Be content in $Be_xZn_{1-x}Se$.

unusual behavior: an increase of frequency with decreasing density of the ZnSe content (see Fig. 5). We suggest that this follows from the positive *TO* phonon dispersion characteristic of bulk binary ZnSe [4]. As can be seen from Fig. 4, all observed modes obey zinc-blende Raman selection rules, which imply a dominance of the *LO* components in *xy* configuration.

Our observation of the two types of BeSe modes indicates that there are two different local arrangements (ordering) of the BeSe bonds in the alloy lattice, and gives evidence of anti-clustering effects in the group-II sublattice [5]. Such effects may be driven by the very large difference in the ZnSe and BeSe bond lengths. We also note that the absence of zinc-blende forbidden components for LO_{2a} and LO_{2b} bands in the Raman spectra[1] is indicative of tetragonal symmetry of the ordered atomic arrangement [6].

References

[1] A. Waag, F. Fischer, H.J. Lugauer, Th. Litz, J. Laubender, U. Lunz, U. Zehneder, W. Ossau, T. Ferhardt, M. Moller, G. Landwehr. Appl. Phys. Lett., **70**, 280 (1997).
[2] J. Gutowski, N. Presser, G. Kudlek. Phys. St. Sol. (a), **120**, 11 (1990).
[3] J.P. Faurie, V. Bousquet, P. Brunet, E. Tournie. J. Cryst. Growth, **184/185**, 11 (1998).
[4] B. Hennion, F. Moussa, G. Pepyand, K. Kunc. Phys. Lett. A, **36**, 377 (1971).
[5] A.M. Mintairov, H. Temkin. Phys. Rev. B, **55**, 5177 (1977).
[6] A.M. Mintairov, P.A. Blagnov, V.G. Melehin, N.N. Faleev, J.L. Merz, Y. Qiu, S.A. Nikishin, H. Temkin. Phys. Rev. B, **56**, 15 836 (1997).

Редактор В.В. Чалдышев

---

[1] The weak structure at 510 cm^{-1} in *xx* configuration is the second order spectra of GaAs substrate.